Conformational Equilibrium of the Reactive Center Loop of Antithrombin Examined by Steady State and Time-Resolved Fluorescence Measurements: Consequences for the Mechanism of Factor Xa Inhibition by Antithrombin−Heparin Complexes†

Akiko Futamura,‡ Joseph M. Beechem,§,|| and Peter G. W. Gettins*,‡

Department of Biochemistry and Molecular Biology, M/C 536, College of Medicine, University of Illinois at Chicago, 1853 West Polk Street, Chicago, Illinois 60612, and Department of Molecular Physiology and Biophysics, Vanderbilt University, Nashville, Tennessee 37232

Received December 26, 2000; Revised Manuscript Received March 28, 2001

ABSTRACT: Activation of antithrombin by high-affinity heparin as an inhibitor of factor Xa has been ascribed to an allosteric switch between two conformations of the reactive center loop. However, we have previously shown that other, weaker binding, charged polysaccharides can give intermediate degrees of activation [Gettins, P. G. W., et al. (1993) *Biochemistry 32*, 8385−8389]. To examine whether such intermediate activation results from different reactive center loop conformations or, more simply, from a different equilibrium constant between the same two extreme conformations, we have used NBD covalently bound at the P1 position of an engineered R393C variant of antithrombin as a fluorescent reporter group and measured fluorescence lifetimes of the label in free antithrombin as well as in antithrombin saturated with long-chain high-affinity heparin, high-affinity heparin pentasaccharide, long-chain low-affinity heparin, and dextran sulfate. Steady state emission spectra, anisotropies, and dynamic quenching measurements were also recorded. We found that the large steady state fluorescence enhancements produced by binding of activators resulted from relief of a static quench of fluorescence of NBD in ∼50% of the labeled antithrombin molecules rather than from any large change in lifetimes, and that similar lifetimes were found for NBD in all activated antithrombin−oligosaccharide complexes. Similar anisotropies and positions of the NBD emission maxima were also found in the absence and presence of activators. In addition, NBD was accessible to quenching agents in both the absence and presence of activators, with an at most 2-fold increase in quenching constants between these two extremes. The simplest interpretation of the partial static quench in the absence of activators, the different degrees of enhancement by different antithrombin activators, and the similar fluorescence properties and quenching behavior of the different states is that there are two distinct types of conformational equilibrium involving three distinct states of antithrombin, which we designate A, A′, and B. A and A′ represent low-affinity or inactive states of approximately equal energy, both having the hinge residues inserted into β-sheet A. A is fluorescent, while A′ is statically quenched. State B represents the activated loop-expelled conformation in which none of the NBD fluorophores are statically quenched, as a result of the loop, including the P1-NBD, moving away from the body of the antithrombin. Different activators are able to shift the equilibrium to the high-activity (B) state to different extents and hence give different degrees of measured activity, and different degrees of relief of static quench. The similar properties and accessibility of the NBD in the A and B conformations also indicate that the P1 side chain is not buried in the low-activity A conformation, suggesting that an earlier proposal that activation involves exposure of the P1 side chain cannot be the explanation for activation. As an alternative explanation, heparin activation may give access to an exosite on antithrombin for binding to factor Xa and hence be the principal basis for enhancement of the rate of inhibition.

The rate of reaction of the inhibitory serpin antithrombin with the target proteinase factor Xa is slow ($<3 \times 10^3$ M^{-1} s^{-1}) and requires physiological activation through binding to the charged polysaccharide heparin. Such activation can give rates of reaction of $>6 \times 10^5$ M^{-1} s^{-1}, representing a physiologically important rate increase of more than 200-fold. Heparin is, however, a heterogeneous polysaccharide, and it was realized long ago that only some heparin sequences bind to antithrombin with high affinity. It was proposed that only high-affinity heparins are active as anticoagulants. Much work led to the identification of a specific heparin pentasaccharide sequence that contains a critical 3-O-sulfated glucosamine residue and that conse-

† Supported by Grant HL49234 (to P.G.W.G.) from the National Institutes of Health.

* To whom correspondence should be addressed. Phone: (312) 996-5534. Fax: (312) 413-0364. E-mail: pgettins@tigger.uic.edu.

‡ University of Illinois at Chicago.

§ Vanderbilt University.

|| Current address: Molecular Probes Inc., Eugene, OR 97402.

10.1021/bi0029346 CCC: $20.00
Published on Web 05/10/2001

quently has high antithrombin affinity ($K_d \sim 50$ nM) (*1*−*3*). Only about one-third of natural heparins, and an even smaller fraction of heparan sulfates, contain this sequence.

A number of spectroscopic techniques have shown that high-affinity heparin (HAH) induces a conformational change in antithrombin (*4*−*6*) and that this conformational change correlates with the large enhancement of the rate of factor Xa inhibition. In addition, kinetic measurements of heparin binding have shown a two-step binding process in which an initial weak binding is followed by an intramolecular step that most probably represents the conformational change that leads to the activated state (*7*). Estimates of the equilibrium constant for the conformational activation indicate that, in the high-affinity heparin-bound state, antithrombin is close to 100% in the highly active conformation ($K = 2600$). Since only a pentasaccharide with the correct 3-*O*-sulfate-containing sequence is needed for high-affinity heparin binding, it was not surprising that both long-chain high-affinity heparin containing this pentasaccharide and the pentasaccharide alone ($K = 800$) (*7*) gave shifts similar to that of the fully activated state when bound to antithrombin and that both appeared to cause the same change in the conformation of the reactive center loop at the P1[1] residue, as monitored by a fluorophore attached at this position (*8*). What was more surprising was our earlier finding that other negatively charged linear polysaccharides can, at saturation, induce a change in the conformation of the reactive center loop of antithrombin and give rise to an intermediate increase in the rate of factor Xa inhibition, even though they do not contain the requisite sequence or composition for high-affinity binding to antithrombin (*8*). The reporter of conformational change at the P1 position in that study was NBD covalently bound to an engineered cysteine at P1. For low-affinity heparin and dextran sulfate binding, only 50 and 20%, respectively, of the enhancement of NBD fluorescence seen with pentasaccharide and HAH was seen. There are two principal possible explanations for this. One is that there are only two reactive center loop conformations for antithrombin, one of very low activity and one of very high activity, and that, depending on the structure of the activating oligosaccharide, a different equilibrium position between these two conformations results from different activators, with consequent intermediate net activation. The second explanation is that different activators induce different final structures for the reactive center loop, each of which has a different activity toward factor Xa. To distinguish between these possibilities, we have used time-resolved fluorescence measurements in this study to obtain the fluorescence lifetimes of the NBD reporter in antithrombin that is free or bound to different activators, as well as steady state emission spectra, anisotropies, and KI quenching data. The results of this study are most simply interpreted in terms of two separate conformational equilibria for antithrombin. The first, between states A and A′, is low-energy (here with NBD attached to P1 the ΔG is ~ 0) and involves a change primarily in the conformation at P1, with the attached fluorophore being fluorescent and exposed in conformation A, but statically quenched and probably inaccessible in conformation A′. For both states, hinge region residues P14 and P15 are inserted into β-sheet A and the activity is low or absent. The second equilibrium is between each of the A states and a fully activated B state in which the hinge residues have been expelled from β-sheet A. While a shift from state A′ to B results in an increased level of exposure of the P1 side chain, there is very little increase in the level of exposure in going from state A to B. Since the exposed A state represents ~50% of the low-activity conformers, a complete shift to 100% B state could cause a greatly increased level of exposure only for the ~50% of A species in the statically quenched A′ conformation and hence give only an ~2-fold enhancement of activity, if such exposure were the basis for allosteric activation. Since instead several hundred-fold activation is seen in the B state, this suggests that there is a different primary explanation for activation of antithrombin than a change in the accessibility of the P1 residue. This is contrary to the current model of allosteric activation of antithrombin by heparin and suggests an alternative in which heparin binding facilitates binding of factor Xa to an exosite on antithrombin, which is in addition to binding of factor Xa to the reactive center loop of antithrombin.

MATERIALS AND METHODS

Production and Purification of R393C Antithrombin. R393C antithrombin was created on a background containing the N135Q mutation that removes one of the potential glycosylation sites and reduces the heterogeneity arising from differences in glycosylation at position 135 (*9*). Site-directed mutagenesis was carried out in M13mp19 using coding strand template 5′-GTGATTGCTGGCTGTCGCTAAAC-CCC-3′ (mutation site underlined). The change was confirmed by dideoxy sequencing. The expression vector, together with selection plasmids pRMH140 and pSV2dhfr, was used to produce stably transfected baby hamster kidney cells. These were grown to confluence in roller bottles, and the level of antithrombin expression was monitored by a radial immunodiffusion assay using commercially available plates containing sheep anti-human antithrombin antibody. The R393C variant antithrombin was purified from pooled serum-free growth medium by chromatography on heparin−Sepharose beads, using a 0.1 to 4 M salt gradient for elution. Fractions containing antithrombin eluted from 1.5 to 2.2 M (low-affinity glycoform) and from 2.2 to 4 M salt (high-affinity glycoform). Since further purification was carried out as part of the NBD labeling, no further purification was carried out at this stage. However, SDS−PAGE showed the preparations to be >95% pure after this single affinity purification step. Pooled fractions were dialyzed overnight against 20 mM sodium phosphate buffer (pH 7.4) containing 0.1 mM EDTA and then concentrated.

To confirm the functional integrity of the variant, the ability to inhibit and form covalent complexes was assayed by SDS−PAGE using the proteinase human neutrophil elastase (neither factor Xa nor thrombin could be used because of the change of the P1 residue from arginine to cysteine). SDS−PAGE carried out under nonreducing conditions showed the presence of only a small amount of disulfide-linked homodimeric antithrombin, though previous experience with this variant has shown that the cysteine at

[1] Abbreviations: P1, P2, etc., designation of residues in the reactive center loop, using the nomenclature of Schechter and Berger (*21*) in which the scissile bond is between residues P1 and P1′, residues N-terminal to this are designated P2, P3, etc., and those C-terminal are designated P2′, P3′, etc.; NBD, *N*,*N*′-dimethyl-*N*-acetyl-*N*′-(7-nitrobenz-2-oxa-1,3-diazol-4-yl)ethylenediamine.

position 393 in the monomeric form is not free, due presumably to disulfide formation with low-molecular weight thiols. SDS−PAGE was carried out in 10% slab gels under either reducing or nonreducing conditions.

Preparation and Purification of NBD-Labeled Antithrombin. Labeling of R393C antithrombin with IANBD was carried out after initial mild and specific reduction with thioredoxin. We have previously shown that thioredoxin used in stoichiometric amounts preferentially reduces any disulfide involving the accessible cysteine 393 rather than any of the structurally important but less accessible internal disulfides of antithrombin (*8*). A mixture with a 1.1:1 molar ratio of thioredoxin to dithiothreitol was incubated for 15 min at room temperature to activate the thioredoxin. The antithrombin to be labeled was bound to heparin−Sepharose beads and the suspension degassed. The cysteine at position 393 was reduced by addition of the reduced thioredoxin to the bead-bound antithrombin, to a stoichiometry of 1:1, and incubation for 30 min at room temperature. A 10-fold molar excess of IANBD was added and the reaction mixture incubated overnight at 4 °C in the dark. Excess reagent was removed by filtration, using a Steriflip Filter unit, and washing with 40 mL of 20 mM sodium phosphate buffer (pH 7.4) containing 1 mM EDTA. The NBD-labeled antithrombin was eluted with 20 mL of 20 mM sodium phosphate buffer (pH 7.4) containing 4 M NaCl and 1 mM EDTA and dialyzed into the same buffer containing 20 mM NaCl.

Specifically labeled active antithrombin was separated from nonspecifically labeled material by heparin affinity chromatography using a linear salt gradient from 0.2 to 3 M. Elution of NBD-labeled antithrombin was monitored using both tryptophan absorption and NBD fluorescence, with the latter using excitation at 480 nm and observing emission at 550 nm. Two major peaks were observed, with the first eluting at the relatively low salt concentration of 1.3 M. The labeled fraction that eluted at normal high salt concentrations (2.0−2.9 M) was taken to be the active fraction. It was suspected that the species with lower affinity resulted from reduction of the cysteine in the heparin binding site involving cysteine 128, since heparin binding to this fraction resulted in a quenching of the NBD fluorescence.

It was found that the NBD-labeled antithrombin was sensitive to freezing and thawing, with a ≥90% loss of activity, judged by loss of the ability of heparin to give enhancement in the NBD fluorescence. Samples used for this study were therefore used immediately after purification and were never frozen.

Stoichiometry of Labeling. The stoichiometry of NBD labeling was determined spectrophotometrically by taking the ratio of the absorbance at 280 and 497 nm and using the extinction coefficient for NBD at 497 nm of 26 000 M^{-1} cm^{-1}. Typical labeling efficiencies of 0.3 mol of NBD/mol of antithombin were obtained. Since all the experiments described herein monitored NBD fluorescence, the low fraction of labeled antithrombin did not affect the results. Indeed, although higher labeling efficiencies could be obtained by using higher ratios of thioredoxin to antithrombin, this also resulted in a greater fraction of inactive material.

Steady State and Time-Resolved Fluorescence Measurements. Steady state fluorescence emission spectra of NBD-labeled R393C antithrombin and its complexes with heparins and dextran sulfate were recorded at 25 °C on an SLM 8000 spectrofluorometer or a SPEX Fluorolog 2 fluorometer. In the case of the SLM8000 apparatus, excitation was at 480 nm, with slits of 4 nm for excitation and 8 nm for emission. Spectra were recorded from 500 to 600 nm in 2 nm steps, with an integration time of 3 s. Spectra were scanned three times to check for reproducibility and averaged. In the case of spectra recorded on the SPEX Fluorolog instrument, excitation was at 480 nm with emission recorded between 490 and 700 nm, with a 0.5 nm increment and a 0.5 s integration time. Antithrombin concentrations were typically 0.9−2 μM. For spectra of complexes of antithrombin and oligosaccharides, the oligosaccharides were added to saturation, which was determined empirically by titration and which was reached at concentrations expected on the basis of previously determined K_d values (*8*). For complexes with high-affinity heparin and heparin pentasaccharide, the oligosaccharide concentration was 5 μM. For low-affinity heparin and dextran sulfate, a concentration of 15 μM was used. Identical conditions were used for measurement of lifetimes and anisotropies.

Fluorescence anisotropy measurements were taken at steady state on a SPEX Fluorolog apparatus employing separate measurements of fluorescence using horizontal and vertical polarizers. For the measurements, we used excitation at 480 nm, with spectra recorded from 490 to 700 nm with 0.5 nm increments and a 0.5 s integration time.

Time-resolved fluorescence measurements were taken with a Coherent Antares neodymium/YAG laser. The output of this laser was frequency-doubled and used to synchronously pump a dual-dye jet laser (Coherent 702) using rhodamine 6G. Output pulses from the dye laser were utilized at 4 MHz and had a pulse width of ∼1 ps. Time-resolved detection utilized time-correlated single-photon counting with a Hamamatsu microchannel plate detector (model R2809U), high-frequency amplifiers (Phillips Scientific model 774), constant-fraction discriminators (Tennelec model 454), time-to-amplitude converters (Tennelec model 862), and pulse-height analysis analog-to-digital converters (Nucleus PCA-II). The instrument response was typically 40−80 ps. The excitation wavelength was 295.5 nm, and emission was collected as a function of time through a 500 nm yellow filter. 8192 data points were collected over a period of 50 ns. Signal averaging was used, with total data collection times of 45−60 min. The sample volume was 150 μL. To estimate the effect of photobleaching, steady state spectra of the sample were recorded before and immediately after each lifetime measurement. No significant photobleaching was observed. Lifetimes and amplitudes were obtained from convoluted multiexponential fits of the data with three separate decays.

Fluorescence Quenching Measurements. Measurements of quenching of NBD fluorescence were carried out on a PTI fluorimeter, with excitation at 480 nm and emission measured at 550 nm, using slits of 4 and 12 nm, respectively. Each measurement was the average of 15 samplings (1 s). For titration with KI, the ionic strength (I) was kept constant at 0.4 by using addition of KI and NaCl stock solutions. The KI stock solution was 0.4 M KI, containing 1 mM $Na_2S_2O_3$ to prevent oxidation of I^-.

Materials. Dextran sulfate was an $M_r = 8000$ species from Sigma. Low- and high-affinity heparins were a generous gift from S. Olson and were prepared as previously described

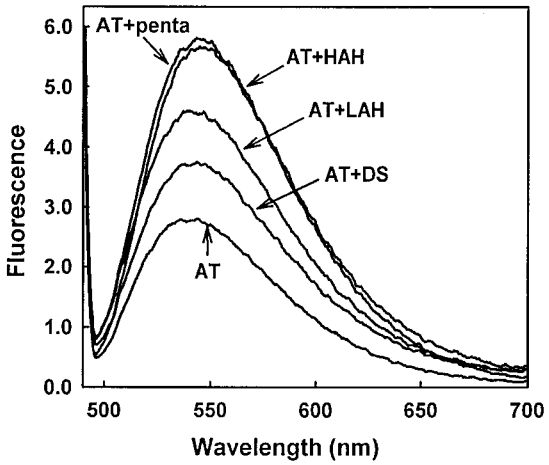

FIGURE 1: Fluorescence emission spectra of NBD-labeled R393C antithrombin: AT, antithrombin alone; AT+DS, antithrombin saturated with dextran sulfate; AT+LAH, antithrombin saturated with low-affinity heparin; AT+PS, antithrombin saturated with heparin pentasaccharide; and AT+HAH, antithrombin saturated with long-chain high-affinity heparin. Saturation was demonstrated separately by a titration of oligosaccharide into labeled antithrombin. The antithrombin concentration in each case was 1 μM.

Table 1: Properties of Steady State Emission Spectra of NBD-Labeled Antithrombin

	emission maximum (nm)	enhancement (%)	anisotropy
antithrombin	542	−	0.245 ± 0.018
antithrombin with pentasaccharide	547	106	0.215 ± 0.012
antithrombin with HAH	548	102	0.214 ± 0.012
antithrombin with LAH	544	62	0.244 ± 0.013
antithrombin with dextran sulfate	544	32	0.236 ± 0.015

(*10*). Thioredoxin was from Sigma. IANBD was from Molecular Probes (Eugene, OR).

RESULTS

Steady State Fluorescence Spectra of NBD-Labeled Antithrombin. Fluorescence emission spectra of R393C antithrombin labeled with IANBD at the P1 cysteine were recorded alone and in the presence of saturating levels of heparin pentasaccharide, high-affinity heparin, low-affinity heparin, and dextran sulfate (Figure 1). The concentration of oligosaccharide needed for saturation was much greater for low-affinity heparin and dextran sulfate because of their lower affinity, and was determined by titration to an end point. As expected from previous experiments (*8*), all of the charged oligosaccharides caused large but varied increases in NBD fluorescence. The largest enhancements (~105%) were caused by heparin pentasaccharide and long-chain high-affinity heparin, whereas low-affinity heparin caused a 62% enhancement and dextran sulfate a 32% enhancement (Table 1). Not previously reported are the wavelength maxima for each of these spectra. In the native state, the maximum was at 542 nm. This was red shifted by ~5−6 nm when high-affinity heparin or heparin pentasaccharide was bound, and by intermediate amounts for dextran sulfate or low-affinity heparin (Table 1). Given the sensitivity of NBD emission spectra to environment, this is a relatively small change and does not suggest a large change in environment such as might occur from changing the P1 side chain from buried to solvent-exposed (*11*).

Fluorescence Anisotropies of Antithrombin and Antithrombin−Oligosaccharide Complexes. Fluorescence anisotropies of the NBD fluorophore were recorded as a function of wavelength for each of the five antithrombin species examined above. Only small differences in anisotropy were seen over the whole spectrum, but these were reproducible and showed a small progressive reduction in anisotropy upon progressing from uncomplexed antithrombin through complexes with dextran sulfate or low-affinity heparin to the pair of complexes with heparin pentasaccharide or high-affinity heparin, indicating only a small reduction in motional constraint upon oligosaccharide binding. Over the range from 525 to 600 nm, which covers the central portion of the emission peak, the average anisotropies were 0.245 for uncomplexed antithrombin and 0.214 for the complex with high-affinity heparin. The complex with heparin pentasaccharide gave an anisotropy almost identical to that with high-affinity heparin, whereas that with low-affinity heparin was 0.244 and with dextran sulfate was 0.236 (Table 1).

Time-Resolved Fluorescence Emission Spectra of NBD-Labeled Antithrombin. To obtain fluorescence lifetimes for free NBD-labeled antithrombin and for NBD in each complex, we recorded time-resolved fluorescence decay intensities, using pulsed excitation of the NBD and signal averaging to give a satisfactory signal-to-noise ratio. The decay curve for NBD-labeled antithrombin did not fit well to a single exponential, but gave an excellent fit to three exponentials, with time constants of 0.13, 0.92, and 6.1 ns (Table 2). Surprisingly, each of the complexes of NBD-labeled antithrombin with oligosaccharides gave an almost identical decay curve (Figure 2), and correspondingly similar, though not quite identical, sets of fluorescence lifetimes. Mean lifetimes, calculated as the sum of the products of normalized amplitude and lifetime, exhibited only small reductions (3−9%) between the value for NBD-labeled antithrombin and the complexes with different oligosaccharides (Table 2). Such decreases in mean lifetime would be expected to result in correspondingly small *decreases* in steady state fluorescence intensity rather than the large increases actually measured. Since steady state fluorescence spectra were recorded on the same samples immediately before and after collection of the decay curves and gave the same large enhancements as reported above, we are confident that the smallness of the changes in lifetime is correct, rather than resulting from any inactivation of the antithrombin. As a separate control, we also examined the change in tryptophan fluorescence of these samples caused by binding each oligosaccharide. In each case, there was the expected enhancement of tryptophan fluorescence, indicating that the antithrombin was in the native state initially and could be converted to an activated state by binding of oligosaccharide. The small reductions in the NBD fluorescence lifetimes, despite large increases in steady state fluorescence, indicate that, in the absence of oligosaccharide, there must be a partial static quench of the NBD fluorescence that is relieved upon activation by binding oligosaccharide (*12*) to account for the large increase in steady state fluorescence intensity. This suggests that there are two distinct low-activity conformations, which we designate A and A′, in one of which (A′) the NBD is statically quenched and the other (A) in which

Table 2: Lifetimes of NBD-Labeled Antithrombin Alone and in Complex with Oligosaccharides[a]

	lifetime 1				lifetime 2				lifetime 3				
species	τ (ns)	α ($\times 10^{3}$)	%	SS%	τ (ns)	α ($\times 10^{3}$)	%	SS%	τ (ns)	α ($\times 10^{3}$)	%	SS%	$\langle\tau_{mean}\rangle$ (ns)
antithrombin	0.130	1.500	41.6	3.4	0.915	1.400	38.7	22.0	6.145	0.742	19.5	74.6	1.612
antithrombin with HAH	0.125	1.800	46.2	3.7	1.001	1.409	35.8	23.1	6.314	0.705	17.9	73.1	1.549
antithrombin with PS	0.116	1.773	45.3	3.5	0.944	1.405	36.8	23.3	6.149	0.670	17.7	73.1	1.491
antithrombin with LAH	0.109	1.770	44.8	3.2	0.927	1.400	36.1	21.4	6.172	0.751	19.0	75.3	1.559
antithrombin with DS	0.090	1.780	44.4	2.7	0.874	1.495	37.1	22.1	5.975	0.741	18.4	75.1	1.465

[a] τ, lifetime; α, amplitude; %, fractional population; SS%, percentage of steady state intensity associated with a given lifetime; $\langle\tau_{mean}\rangle$, mean lifetime calculated as the sum of fractional populations $\times$ τ_i.

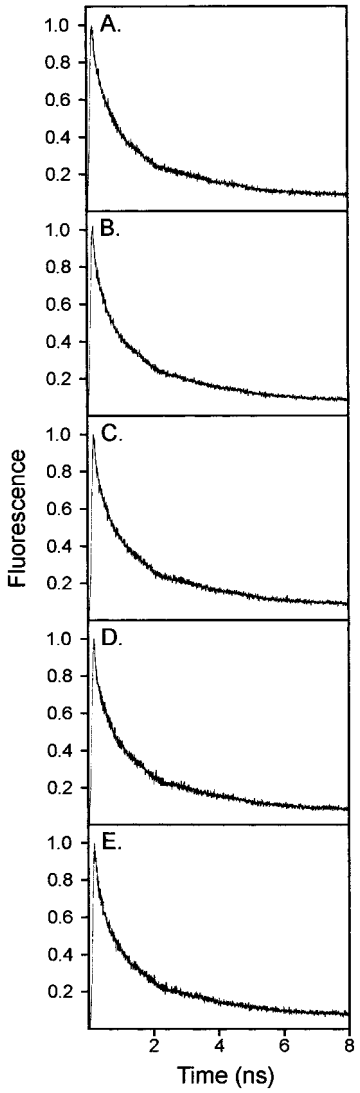

FIGURE 2: Fluorescence decay curves for NBD-labeled antithrombin and antithrombin−oligosaccharide complexes, monitored at ≥500 nm: (A) NBD-labeled antithrombin, (B) complex with high-affinity heparin, (C) complex with low-affinity heparin, (D) complex with dextran sulfate, and (E) complex with heparin pentasaccharide. The antithrombin concentrations were 2 μM, and the oligosaccharide concentrations were 5 μM pentasaccharide, 5 μM high-affinity heparin, 15 μM low-affinity heparin, and 15 μM dextran sulfate.

it is fluorescent. Since these states must be populated about 50:50 in the present P1-NBD derivative to account for the ~100% fluorescence enhancement upon full activation, this suggests a ΔG of ~0 kcal/mol. In wild-type antithrombin where P1 is an arginine or in other natural variants (where P1 is histidine), the energy difference might be slightly greater, as a result of additional binding to a negative charge on the serpin body. However, as indicated in the accompanying paper (*13*), the increase in heparin affinity for the P1 histidine variant in the uncharged state is small, suggesting that the ΔG between A and A′ conformations would also be small and the population difference between A and A′ conformations still not be very much in favor of the inaccessible A′ conformation.

Dynamic Quenching. As a further way of examining the change in environment of the NBD moiety upon heparin binding to antithrombin, we examined the effect of added quencher on NBD fluorescence. Acrylamide was found to have a negligible effect (data not shown), whereas KI was an effective quencher of NBD fluorescence in both the absence and presence of heparin, but more so in the heparin-bound state. NBD in both the antithrombin−pentasaccharide and antithrombin−HAH complexes exhibited indistinguishable behavior. Estimates of the quenching constants of heparin-complexed and uncomplexed antithrombin−NBD species, determined from the slope of Stern−Volmer plots (Figure 3), gave values of 4.2−4.4 M^{-1} (for high-affinity heparin and pentasaccharide) and 2.6 M^{-1}, respectively. The upward curvature in the Stern−Volmer plot at high KI concentrations for high-affinity heparin− and pentasaccharide−antithrombin complexes most probably results from specific competition of I^- for the heparin binding site that has been previously reported (*5*). Accordingly, estimates of the quenching constants were made from the initial, more linear parts of the plot. While the values of 4.2−4.4 and 2.6 M^{-1} differ well beyond experimental error, they indicate that the NBD is already considerably exposed to solvent in the unactivated state, and becomes only slightly more exposed upon heparin binding. Measurements were not taken for complexes with the much weaker binding oligosaccharides, since the further weakening of affinity for antithrombin caused by the high ionic strength and specific competition by I^- made it difficult to ensure saturation of the antithrombin with the charged oligosaccharide.

DISCUSSION

We have used a combination of steady state and time-resolved fluorescence measurements on an NBD fluorophore linked to an engineered cysteine at the P1 position of antithrombin to help distinguish between two very different models of conformational change induced in the reactive center loop of antithrombin by allosteric activators. One model proposes only two conformations for the reactive center loop, A and B, with A being of very low activity with respect to inhibition of factor Xa, and B being maximally active. On this model, allosteric activators of antithrombin produce different degrees of activation when bound in a 1:1

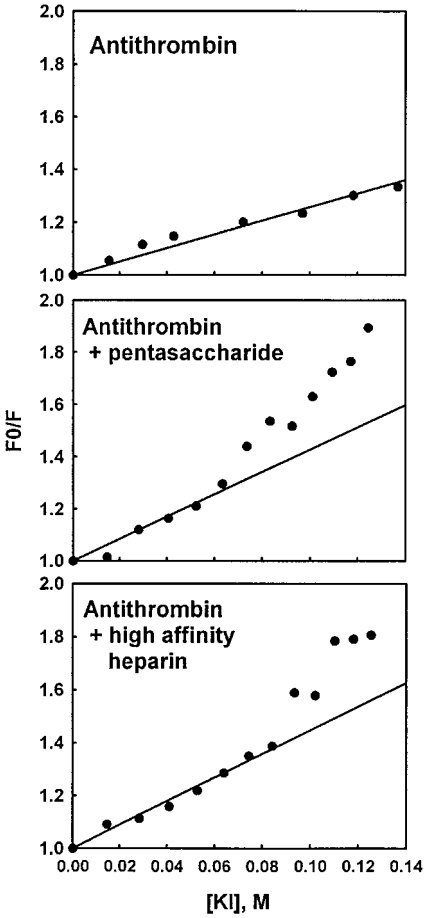

FIGURE 3: Stern−Volmer plot of quenching by KI of NBD fluorescence of NBD-labeled antithrombin in the absence and presence of bound heparin. The ionic strength was maintained at 0.4 throughout.

complex, as a result of producing different equilibrium populations of A and B. The second model proposes that each different activator produces a different conformation for the reactive center loop with a different activity for inhibition of factor Xa. Our findings of similar lifetimes, anisotropies, and emission maxima of both unactivated antithrombin and antithrombin activated by various oligosaccharide species, together with the existence of a partial static quench in the inactive state, are most simply interpreted in terms of a slightly modified version of the first, two-state, model. The modification is that in the low-activity state there must be a second equilibrium between two approximately equally populated conformations, A and A′, that differ primarily in the interaction of the P1 side chain (here NBD) with the body of the serpin and hence in whether here the NBD fluorescence is statically quenched or not. The surprising finding that the solvent exposure and degree of motional constraint of the NBD fluorophore in the unactivated (A) and activated (B) conformations do not differ dramatically suggests that increased accessibility of the P1 residue to proteinase or increased conformational flexibility is not likely to be the basis for the very large activation of antithrombin as an inhibitor of factor Xa in the B conformation. This is contrary to what has previously been proposed on the basis of the properties of a P1 histidine variant of antithrombin in native and heparin-activated states and of reactivity of the P1 arginine of wild-type antithrombin to a modifying enzyme (*14*).

Given the approximate doubling in fluorescence intensity of NBD attached to the antithrombin P1 position upon binding high-affinity heparin, we had expected that the mean fluorescence lifetimes would show a comparable large change (i.e., an approximately 2-fold increase). This was not what we found. Instead, while there was a statistically significant change in mean lifetimes between the native and heparin-complexed states (Table 2), it was a *reduction* of 3−9% rather than an increase of up to 100%, and so cannot at all account for the observed increases in steady state fluorescence for each of the complexes. The observed behavior is, instead, what is expected from the existence of a partial static quench (*12*) of the NBD fluorophore in the native state that is relieved upon heparin binding and consequent conformational change in the reactive center loop. In terms of the structure of antithrombin, this can be interpreted as the P1 position in the native state being close to the body of the serpin (*15*), a position in which the NBD fluorophore could interact with residue(s) on the surface in such a way as to be statically quenched. Since NBD in this state is not completely silent, however, it is necessary to propose only a partial quench, which could arise from two different orientations of the NBD, of approximately equal energy and hence population (A and A′), one of which is statically quenched (A′) and the other not (A). When heparin binds, which is known to result in expulsion of the hinge of the reactive center loop (residues P15 and P14) from β-sheet A (*16*) and presumably allows greater motional freedom for the remainder of the reactive center loop, including P1, the NBD attached to P1 could move away from the serpin body and thereby relieve the static quench. The observed large enhancement in fluorescence would then be due to (i) relief of the static quench causing a large increase in fluorescence as A′ conformations are converted to B and (ii) a small reduction in the fluorescence lifetime in the new conformation opposing this with a small *decrease* in fluorescence as exposed A conformations are converted to B (Table 2).

Such small reductions in mean NBD fluorescence lifetimes between the two states that represent close to 100% in the inactive conformation (native antithrombin) and close to 100% in the fully active conformation (complexes with pentasaccharide and high-affinity heparin) also explain why analysis of the decay curves of complexes with low-affinity heparin and dextran sulfate gave similar reductions in lifetime rather than well-resolved contributions from each of the two extreme states that were present. Equally, for the steady state anisotropies, a weighted average would be observed, which would lie between those of the two extreme conformations. However, while these observations could also be explained by a multiple-conformation model, such an explanation would require that such closely similar multiple conformations be recognized sufficiently differently by factor Xa to result in the observed large differences in inhibitory activity, which seems very unlikely.

With relief of static quenching as the explanation for reconciling the small measured decrease in mean fluorescence lifetime with a large increase in fluorescence intensity upon heparin binding, the need to explain why the heparin-induced conformational change does not greatly alter the lifetime of NBD at the P1 position arises, since the working hypothesis for heparin activation of antithrombin toward inhibition of factor Xa has been a large heparin-induced

change in the environment and/or accessibility of the P1 residue (*14*) to better fit the active site of the proteinase (*17*). Here it is significant that our earlier fluorescence study, which demonstrated conformational change at the P1 position of antithrombin in response to heparin binding, had screened several potential fluorophore reporter groups for the P1 position, but found that only NBD was sufficiently responsive to be a sensitive reporter. The others (fluorescein, pyrene, dansyl, and ANS) gave either no change in fluorescence upon heparin binding or only a small (<10%) increase or decrease (*8*). At that time, the consequences of this insensitivity were not considered in detail. However, that finding, and the small changes in mean fluorescence lifetime, in anisotropy, in wavelength maximum, and in the level of dynamic quenching for the steady state emission spectra of the NBD examined here, all suggest that the surroundings of the P1 side chain (as reported by the NBD fluorophore) do not change dramatically in nature between the two states, and also involve ready access to solvent in both states. Thus, the wavelength maximum of the NBD of 542 nm in the native state compared with a maximum of 550 nm for free IANBD suggests an environment not greatly altered from that of NBD free in solution. It further compares with a much lower wavelength maximum of ~529 nm in more hydrophobic but still partially solvent-accessible surroundings (*11*). Upon heparin-induced expulsion of the reactive center loop hinge of antithrombin, there is a red shift of 5−6 nm in the NBD wavelength maximum, making it almost the same as that for free IANBD. This is accompanied by a small reduction in anisotropy, suggesting a small reduction in local constraints, and a small reduction in fluorescent lifetimes. Finally, quenching by I^- occurs in both native and loop-expelled conformations with at most an only 2-fold change in the quenching constant. Given such small observed changes for the intrinsically sensitive NBD, it is now apparent why the less environmentally sensitive fluorophores examined in our earlier study were much less responsive to heparin binding. Another paper (*18*) comes to the same conclusion from examination of the properties of a P1W variant of antithrombin.

The conclusion that heparin binding to antithrombin, though probably resulting in movement of the P1 residue away from the body of the serpin, does not greatly alter the solvent accessibility or motional freedom of the P1 side chain in the well-populated A conformation is not what we had expected on the basis of the current working model for the mechanism of heparin activation of antithrombin. This model posits that heparin-induced conformational change in the reactive center loop, most specifically at and adjacent to the proteinase recognition site of the P1−P1′ bond, involves a major increase in accessibility and/or backbone flexibility that allows factor Xa to recognize the scissile bond as a better substrate and hence results in a large enhancement in the rate of inhibition by the heparin-activated antithrombin. While heparin binding does result in a change in the environment of the A′ conformation antithrombin molecules (~50%), this is only likely to result in an ~2-fold increase in the rate of reaction, as is seen for allosteric activation of thrombin inhibition. Instead, the current findings strongly suggest that there must be some additional, probably dominant, factor that contributes to the enhancement in the rate of the antithrombin−factor Xa reaction. A possibility is that a new exosite−exosite interaction between antithrombin and factor Xa occurs, involving residues on antithrombin beyond P1 and possibly outside of the reactive center loop and either made accessible to the exosite on factor Xa through expulsion of the reactive center loop (to which factor Xa would be bound at its active site) from β-sheet A of the antithrombin or formed through a heparin-induced conformational change within the body of antithrombin. The plausibility of such exosite−exosite interactions being important for factor Xa inhibition is supported by the demonstrated mechanism of inhibition of factor Xa by two parasite inhibitors, TAP and antistasin (*19*, *20*). Each of these uses an exosite on factor Xa for a major portion of the binding energy. We propose that such an exosite on antithrombin, made available through heparin-induced conformational change, is also a major contributor to factor Xa binding and hence to the rate of inhibition. Independent experimental evidence in support of this proposal comes from mutagenesis studies on the reactive center loop of antithrombin, which indicate that a determinant outside of the reactive center loop is critical for much of the rate enhancement of factor Xa inhibition (*18*).

ACKNOWLEDGMENT

We thank Steven Olson (University of Illinois at Chicago) for generously supplying low- and high-affinity fractionated heparins and for helpful comments on the manuscript.

REFERENCES

1. Lindahl, U., Bäckström, G., Thunberg, L., and Leder, I. G. (1980) *Proc. Natl. Acad. Sci. U.S.A. 77*, 6551−6555.
2. Choay, J., Petitou, M., Lormeau, J. C., Sinaÿ, P., Casu, B., and Gatti, G. (1983) *Biochem. Biophys. Res. Commun. 116*, 492−499.
3. Atha, D. H., Stephens, A. W., and Rosenberg, R. D. (1984) *Proc. Natl. Acad. Sci. U.S.A. 81*, 1030−1034.
4. Björk, I., Danielsson, Å., Fish, W. W., Larsson, K., Lieden, K., and Nordenman, B. (1979) in *The physiological inhibitors of coagulation and fibrinolysis* (Collen, D., Wiman, B., and Verstraete, M., Eds.) pp 67−84, Elsevier/North-Holland, Amsterdam.
5. Olson, S. T., and Shore, J. D. (1981) *J. Biol. Chem. 256*, 11065−11072.
6. Gettins, P. (1987) *Biochemistry 26*, 1391−1398.
7. Olson, S. T., Björk, I., Sheffer, R., Craig, P. A., Shore, J. D., and Choay, J. (1992) *J. Biol. Chem. 267*, 12528−12538.
8. Gettins, P. G. W., Fan, B., Crews, B. C., Turko, I. V., Olson, S. T., and Streusand, V. J. (1993) *Biochemistry 32*, 8385−8389.
9. Turko, I. V., Fan, B., and Gettins, P. G. W. (1993) *FEBS Lett. 335*, 9−12.
10. Streusand, V. J., Björk, I., Gettins, P. G. W., Petitou, M., and Olson, S. T. (1995) *J. Biol. Chem. 270*, 9043−9051.
11. Shore, J. D., Day, D. E., Francis-Chmura, A. M., Verhamme, I., Kvassman, J., Lawrence, D. A., and Ginsburg, D. (1995) *J. Biol. Chem. 270*, 5395−5398.
12. Lakowicz, J. R. (1999) in *Principles of Fluorescence Spectroscopy*, 2nd ed., p 242, Kluwer Academic, New York.
13. Chuang, Y.-J., Swanson, R., Raja, S., Bock, S. C., and Olson, S. T. (2001) *Biochemistry 40*, 6670−6679.
14. Pike, R. N., Potempa, J., Skinner, R., Fitton, H. L., McGraw, W. T., Travis, J., Owen, M., Jin, L., and Carrell, R. W. (1997) *J. Biol. Chem. 272*, 19652−19655.
15. Carrell, R. W., Stein, P. E., Fermi, G., and Wardell, M. R. (1994) *Structure 2*, 257−270.

16. Huntington, J. A., Olson, S. T., Fan, B., and Gettins, P. G. W. (1996) *Biochemistry 35*, 8495−8503.
17. Chuang, Y.-J., Gettins, P. G. W., and Olson, S. T. (1999) *J. Biol. Chem. 274*, 28142−18149.
18. Chuang, Y. J., Swanson, R., Raja, S. M., and Olson, S. T. (2001) *J. Biol. Chem. 276*, 14961−14971.
19. Wei, A. Z., Alexander, R. S., Duke, J., Ross, H., Rosenfeld, S. A., and Chang, C. H. (1998) *J. Mol. Biol. 283*, 147−154.
20. Mao, S. S., Przysiecki, C. T., Krueger, J. A., Cooper, C. M., Lewis, S. D., Joyce, J., Lellis, C., Garsky, V. M., Sardana, M., and Shafer, J. A. (1998) *J. Biol. Chem. 273*, 30086−30091.
21. Schechter, I., and Berger, A. (1967) *Biochem. Biophys. Res. Commun. 27*, 157−162.

BI0029346